

## Thermal conductivity of a shearing fluid

Peter J. Daivis and Denis J. Evans

*Research School of Chemistry, Australian National University, G.P.O. Box 4, Canberra 2601, Australia*

(Received 22 December 1992)

A recently derived Green-Kubo formula for the thermal conductivity of a shearing fluid has been used to calculate the thermal conductivity of a strongly shearing Lennard-Jones fluid in the limit of zero temperature gradient. Using nonequilibrium molecular-dynamics simulation methods, we find that the diagonal elements of the thermal-conductivity tensor are independent of the strain rate  $\gamma$  up to approximately  $\gamma=1.0$ . At higher strain rates, the  $xx$  and  $yy$  elements increase weakly with strain rate while the  $zz$  element decreases weakly. The  $xy$  and  $yx$  elements of the thermal-conductivity tensor decrease, initially linearly, with increasing strain rate from their equilibrium value of zero. These results are in agreement with conclusions obtained from symmetry arguments.

PACS number(s): 66.60.+a, 05.60.+w, 83.50.Sp

### I. INTRODUCTION

A consequence of the theory of linear nonequilibrium thermodynamics is that couplings between fluxes and forces of different tensorial rank such as the heat-flux vector and the strain-rate tensor are forbidden [1]. Furthermore, the phenomenological coefficients are assumed to be independent of the thermodynamic forces, so the thermal conductivity is taken to be independent of both the temperature gradient and the strain rate in a weakly shearing fluid. When the thermodynamic forces are large, these assumptions are no longer valid. The material may become anisotropic under the influence of strong thermodynamic forces. Nonlinear constitutive relations introduce the possibility of couplings that are not present in the linear theory and the transport coefficients may become dependent on the thermodynamic forces.

Two methods have commonly been used to calculate the linear thermal conductivity by computer simulation. One is to evaluate the well-known Green-Kubo formula relating the thermal conductivity to the correlation of fluctuations in the heat-flux vector in an equilibrium system. The other is to perform nonequilibrium molecular-dynamics (NEMD) simulations in which a synthetic "heat field" is used to generate a heat flux. The thermal conductivity can then be obtained by extrapolating the flux-force ratio to zero field, giving the linear thermal conductivity.

In previous work, we [2] have shown that the Green-Kubo method can be extended to a strongly shearing fluid, giving the strain-rate-dependent zero-temperature-gradient limit of the thermal-conductivity tensor. It has also been shown that no simple, efficient NEMD method exists for calculating this quantity [3].

In this paper, we use the Green-Kubo formula derived previously to calculate the thermal-conductivity tensor  $\lambda$  as a function of strain rate in a strongly shearing atomic fluid.

### II. GREEN-KUBO RELATION

The linear thermal conductivity is defined by the linear constitutive relation for heat flow (Fourier's law)

$$\mathbf{J}_E(\mathbf{r}, t) = -\lambda \cdot \nabla T(\mathbf{r}, t), \quad (1)$$

where  $\mathbf{J}_E(\mathbf{r}, t)$  is the heat-flux vector in the Eulerian picture of hydrodynamics in which each hydrodynamic variable is a function of the position vector  $\mathbf{r}$  and the time  $t$ . In general, the thermal conductivity is a second-rank tensor. This is important when considering anisotropic materials. The linear thermal conductivity of an isotropic fluid reduces to a scalar given by the well-known Green-Kubo relation [4,5]

$$\lambda = \frac{V}{3k_B T^2} \int_0^\infty dt \langle \mathbf{J}_E(t) \cdot \mathbf{J}_E(0) \rangle_0, \quad (2)$$

where  $\mathbf{J}_E(t)V$  is the zero wave-vector limit of the Fourier transform of  $\mathbf{J}_E(\mathbf{r}, t)$ . The 0 subscript indicates that the average is carried out at equilibrium. The microscopic expression for  $\mathbf{J}_E(t)V$  is

$$\mathbf{J}_E(t)V = \sum_i \frac{\mathbf{p}_i}{m} e_i - \frac{1}{2} \sum_{i,j (\neq i)} \mathbf{r}_{ij} \mathbf{F}_{ij} \cdot \frac{\mathbf{p}_i}{m}, \quad (3)$$

where  $\mathbf{p}_i$  is the momentum of particle  $i$ ,  $m$  is the particle mass,  $\mathbf{r}_{ij}$  is equal to  $\mathbf{r}_j - \mathbf{r}_i$ ,  $\mathbf{F}_{ij}$  is the force on particle  $i$  due to particle  $j$ , and  $V$  is the volume of the system. Equation (2) is evaluated at equilibrium, so the time-averaged fluid velocity  $\mathbf{u}(\mathbf{r})$  is zero. In this case, the internal energy per particle  $e_i$  is given by

$$e_i = \frac{p_i^2}{2m} + \frac{1}{2} \sum_{j (\neq i)} \phi_{ij}, \quad (4)$$

where  $\phi_{ij}$  is the potential energy of particle  $i$  due to interaction with particle  $j$ .

Now consider an atomic liquid subjected to steady homogeneous shear with an average streaming velocity given by  $\mathbf{u}(\mathbf{r}) = \mathbf{i}\gamma y$  where  $\mathbf{i}$  is a unit vector in the  $x$  direction and  $\gamma$  is the strain rate. Such a system can be described by the Slod equations of motion [5] (so named because of their close relationship to the Dolls tensor algorithm)

$$\begin{aligned}\dot{\mathbf{r}}_i &= \frac{\mathbf{p}_i}{m} + i\gamma y_i, \\ \dot{\mathbf{p}}_i &= \mathbf{F}_i - i\gamma p_{iy} - \alpha \mathbf{p}_i,\end{aligned}\quad (5)$$

where, at low Reynolds number,  $\mathbf{p}_i$  is now the peculiar momentum of particle  $i$ , defined as  $m[\mathbf{v}_i - \mathbf{u}(\mathbf{r}_i)]$ , and  $\mathbf{F}_i = \sum_j \mathbf{F}_{ij}$ .  $\alpha$  is a coefficient determined from Gauss's principle of least constraint that makes the kinetic temperature or total energy of the system a constant of the motion.

Due to symmetry considerations, the shear cannot induce a heat flow in this system, but it can affect the thermal conductivity, which now becomes a tensor.

Two descriptions of hydrodynamics are commonly used. One is the Eulerian description in which the hydrodynamic variables are specified at a given time and a fixed point in space. The other is the Lagrangian description, in which the hydrodynamic variables are specified at a given time and a particular point moving with the fluid. Evans [2] has shown that it is possible to derive a Green-Kubo relation for elements of the strain-rate-dependent thermal-conductivity tensor. In this derivation, microscopic Lagrangian coordinates  $\mathbf{q}_i$  are introduced where

$$\begin{aligned}\mathbf{q}_i(t) &= \mathbf{r}_i(0) + \int_0^t \frac{\mathbf{p}_i(s)}{m} ds \\ &= \mathbf{r}_i(t) - \int_0^t \mathbf{u}_i(s) ds.\end{aligned}\quad (6)$$

Note that at time  $t=0$ , we have  $\mathbf{q}_i(0) = \mathbf{r}_i(0)$ . These microscopic Lagrangian coordinates are analogous to the macroscopic Lagrangian coordinates used in fluid dynamics. However, there is an important difference between the two. In the macroscopic case, a point in the Lagrangian coordinate system moves with the fluid at the local macroscopic fluid velocity. In the case of planar shear flow, the macroscopic fluid velocity has only an  $x$  component, and it is not possible for a fluid "particle" to move from one streamline to another. In the microscopic case, this is not so. The velocity of a given particle consists of a thermal part and a streaming part. The thermal component (represented by the Slod momentum  $\mathbf{p}_i$ ) allows a molecule to move from one streamline to another. For the streaming component of the displacement to be completely removed, allowance must be made for a variation in the local streaming velocity experienced by the molecule, as is done in Eq. (6). This is easily seen when  $\mathbf{u}_i = i\gamma y_i$  is substituted into Eq. (6), giving

$$\mathbf{q}_i(t) = \mathbf{r}_i(t) - i\gamma \int_0^t y_i(s) ds. \quad (7)$$

The microscopic Lagrangian internal energy density is given by

$$e(\mathbf{q}, t) = \sum_i e_i(t) \delta(\mathbf{q} - \mathbf{q}_i(t)). \quad (8)$$

This leads to the following expression for the zero-wave-vector Lagrangian heat-flux vector [2]:

$$\mathbf{J}_L(t)V = \sum_i \frac{\mathbf{p}_i}{m} e_i - \frac{1}{2} \sum_{i,j(i \neq j)} \mathbf{q}_{ij} \mathbf{F}_{ij} \cdot \frac{\mathbf{p}_i}{m}. \quad (9)$$

The thermal-conductivity tensor is defined in terms of a linear constitutive relation between the Lagrangian heat-flux vector and the gradient of the Lagrangian internal energy density fluctuation. The use of a linear constitutive equation is valid because the internal energy density gradients are assumed to be small. After Fourier transforming with respect to  $\mathbf{q}$  and Fourier-Laplace transforming with respect to  $t$ , the result

$$\mathbf{J}_L(\mathbf{k}, \omega) = \frac{\lambda(\mathbf{k}, \omega)}{\rho c_v} \cdot i\mathbf{k}e(\mathbf{k}, \omega) \quad (10)$$

is obtained. This is simply the  $\mathbf{k}$  and  $\omega$  space version of a generalization of Eq. (1) that allows for spatial and temporal memory in the Lagrangian frame. Note that the constant volume specific heat arises from the fact that we have expressed the constitutive equation in terms of internal energy gradients rather than temperature gradients. A derivation very similar to that used to obtain the equilibrium thermal conductivity [2] leads to the final result for the thermal-conductivity tensor [5]

$$\lambda = \frac{V}{k_B T_e^2} \int_0^\infty dt \langle \mathbf{J}_L(t) \mathbf{J}_L(0) \rangle_\gamma. \quad (11)$$

Here,  $\langle \rangle_\gamma$  denotes an average over an equilibrium canonical ensemble of systems that have been brought into a shearing steady state using constant energy dynamics. It is assumed that the strain rate was applied at time  $t = -\infty$  and that a steady state has been achieved by the time  $t = 0$ . Note that a canonical ensemble of systems that have been brought into a shearing steady state using constant energy dynamics has the same energy fluctuations as the equilibrium ensemble from which it was generated. This means that the zero time value of the correlation function of internal energy density fluctuations is the same as it is at equilibrium. This, in turn, is related to the specific heat and the temperature  $T_e$  of the generating equilibrium ensemble. Therefore the temperature appearing in Eq. (11) is the equilibrium temperature, not the kinetic temperature of the nonequilibrium steady state [2]. Note that, at equilibrium, Eq. (11) reduces to Eq. (2).

### III. SIMULATION DETAILS

The homogeneous shear NEMD method was used to simulate planar Couette flow, using the equations of motion given in Eq. (5). A constant kinetic temperature thermostat with  $\alpha$  in Eq. (5) given by

$$\alpha = \frac{\sum_i (\mathbf{F}_i \cdot \mathbf{p}_i - \gamma p_{xi} p_{yi})}{\sum_i p_i^2} \quad (12)$$

was used for equilibrium simulations and a constant energy thermostat with  $\alpha$  given by

$$\alpha = \frac{-\gamma P_{yx}(t)V}{\sum_i p_i^2/m} \quad (13)$$

where  $P_{yx}$  is the  $yx$  element of the pressure tensor, was

used for some equilibrium and all nonequilibrium simulations. Linear proportional feedback was used to cancel the small drift in temperature or energy introduced by the finite numerical accuracy of the differential-equation solver and the finite floating-point representation of numbers. The same method has previously been used to compensate for the drift in bond length constraints due to numerical errors in simulations of rigid molecules [6].

Equation (9) shows that both the laboratory position and the Lagrangian position of each particle are needed for calculations of the heat-flux vector and the thermal-conductivity tensor. In NEMD simulations of planar Couette flow, periodic boundary conditions that are compatible with the shear are necessary. Lees-Edwards (sliding brick) boundary conditions are usually used. However, different periodic boundary conditions are required for the Lagrangian coordinates, because they are calculated from "shear-free" equations of motion. This is easily seen by taking the time derivative of Eq. (6). Therefore both shearing and shear-free periodic boundary conditions are required.

The correlation functions were calculated by creating a "shift register" of values of  $\mathbf{J}_L$ ,  $\tau_s$  reduced time units long. When the shift register was filled, a correlation function was calculated by multiplying the time zero value by the subsequent values. Then the Lagrangian coordinates were reset to equal the laboratory coordinates, the shift register was refilled, and another correlation function calculated. This method differs from the usual way of calculating correlation functions at equilibrium, in which the values of the observable are simply shifted and the first value in the shift register taken as the time zero value. It is also less efficient, because each correlation function accumulation is performed after  $\tau_s$  time steps instead of after each shift register update. However, it was necessary to calculate the correlation functions in this way because of the explicit appearance of the time origin in the definition of the Lagrangian coordinates. In practice, it was found convenient to split the correlation functions into those parts that could be accumulated at each shift register update, and those that could only be accumulated every  $\tau_s$  time steps.

The simulated system was a Lennard-Jones fluid with a potential given by

$$\phi = 4\epsilon \left[ \left( \frac{r}{\sigma} \right)^{-12} - \left( \frac{r}{\sigma} \right)^{-6} \right], \quad (14)$$

with  $\epsilon$  and  $\sigma$  set equal to 1. The potential was truncated at  $2.5\sigma$  and shifted so that the potential was zero at the point of truncation. The reduced temperature was 2.0 and the reduced density was 0.8, corresponding to a supercritical fluid. This state point was chosen because the linear thermal conductivity of this system has been calculated previously from nonequilibrium molecular-dynamics simulations [7]. All results are expressed in reduced units, with  $\sigma$  the unit of length,  $m$  the unit of mass, and  $\epsilon$  the unit of energy.

From the equilibrium simulations, the average reduced internal energy per particle was calculated to be  $-0.8979$ . Equation (11) was then used to evaluate the

thermal conductivity of a Lennard-Jones fluid as a function of strain rate at reduced density  $\rho=0.8$  and reduced internal energy per particle of  $-0.8979$ . The correlation function was evaluated as a time average over a trajectory at fixed internal energy equal to the average internal energy of the constant temperature equilibrium system. This differs slightly from Eq. (11) in which the ensemble average is over an initial equilibrium canonical ensemble of systems that are brought into a shearing steady state using constant energy dynamics, but we do not expect this to have an effect on the results [9].

The equations of motion were solved using a Gear predictor-corrector algorithm with a reduced time step of 0.002. The results quoted here were typically the result of an average over three runs, each of  $8 \times 10^6$  time steps (or  $1.6 \times 10^4$  reduced time units).

#### IV. RESULTS AND DISCUSSION

The values of the linear thermal conductivity  $\lambda$  obtained from an equilibrium simulation at constant kinetic temperature using Eq. (2) was  $7.38 \pm 0.3$ . Nonequilibrium simulations at constant kinetic temperature using the following equations of motion [5]:

$$\begin{aligned} \dot{\mathbf{r}}_i &= \frac{\mathbf{p}_i}{m}, \\ \dot{\mathbf{p}}_i &= \mathbf{F}_i + (e_i - \bar{e})\mathbf{F}_Q(t) - \frac{1}{2} \sum_{j=1}^N \mathbf{F}_{ij} [\mathbf{r}_{ij} \cdot \mathbf{F}_Q(t)] \\ &\quad + \frac{1}{2N} \sum_{j,k} \mathbf{F}_{jk} [\mathbf{r}_{ij} \cdot \mathbf{F}_Q(t)] - \alpha \mathbf{p}_i, \end{aligned} \quad (15)$$

with a heat field  $F_{Qz}$  of 0.2, give  $\lambda=7.17$ . Both of these values are in good agreement with the results of Evans [7], who found a linear thermal conductivity extrapolated to zero heat field of  $7.25 \pm 0.1$ , and a negligible dependence of  $\lambda$  on the heat field  $F_Q$  up to  $F_Q=0.2$ .

Equation (11) for the thermal-conductivity tensor of a shearing fluid can be written in the form

$$\begin{aligned} \lambda &= \frac{V}{k_B T_e^2} \int_0^\infty dt \langle \mathbf{J}_E(t) \mathbf{J}_E(0) + \mathbf{J}'(t) \mathbf{J}_E(0) \rangle_\gamma \\ &= \frac{V}{k_B T_e^2} \int_0^\infty [\mathbf{C}_E(t) + \mathbf{C}'(t)] dt \\ &= \lambda_E + \lambda', \end{aligned} \quad (16)$$

where  $\mathbf{J}'(t) = \mathbf{J}_L(t) - \mathbf{J}_E(t)$  and we have used the fact that  $\mathbf{J}_L(0) = \mathbf{J}_E(0)$ . When  $\mathbf{u}(\mathbf{r}) = i\gamma y$ ,  $\mathbf{J}'(t)$  can be written explicitly as

$$\mathbf{J}'(t)V = \frac{1}{2} \sum_{i,j (\neq 1)} i\gamma \left[ \int_0^t y_{ij}(s) ds \right] \mathbf{F}_{ij} \cdot \frac{\mathbf{p}_i}{m}. \quad (17)$$

This term can be seen as a contribution to the energy flux due to the convective motion induced by the shear and it must be subtracted to find the diffusive energy flux. Note that it is zero for those particles whose  $y$  coordinates are equal for the interval 0 to  $t$ .

Elements of the correlation function tensor  $\mathbf{C}_E(t)$  evaluated at a strain rate of  $\gamma=2.0$  are shown in Fig. 1. The

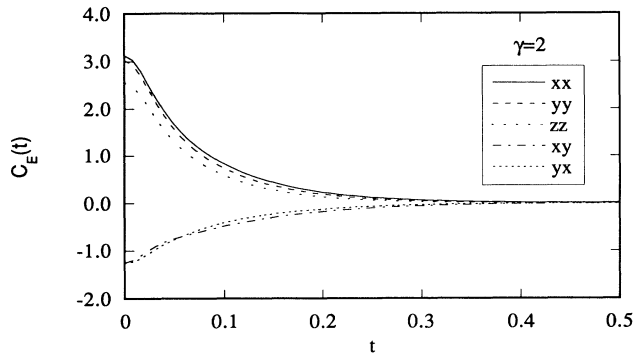


FIG. 1. Diagonal and off-diagonal elements of the correlation function tensor  $\mathbf{C}_E(t)$  at a strain rate of  $\gamma=2.0$ . Elements not shown were zero within errors. The functions were evaluated at a reduced time of 1.0, but were essentially zero in the interval 0.5 to 1.0.

diagonal elements are positive and the off-diagonal elements are negative. The off-diagonal elements not plotted were equal to zero within experimental errors. Elements of the correlation function tensor  $\mathbf{C}'(t)$  evaluated at a strain rate of  $\gamma=2.0$  are shown in Fig. 2. Figure 2 shows that only the  $xx$  and  $xy$  elements of the thermal-conductivity tensor are affected by the distinction between  $\mathbf{r}_{ij}$  and  $\mathbf{q}_{ij}$ . It is apparent that these correlation functions become very noisy at long times. This is due to the fact that  $\mathbf{q}_{ij}$  becomes large on the time scale required for the calculation of the correlation functions because particles close enough to interact at time  $t$  may have had very different initial positions and therefore streaming velocities at time  $t=0$ . The time taken for particles to sample all streaming velocities is related to the time for a particle to diffuse from the top of the box to the bottom. Another reason for the larger noise amplitude in the  $\mathbf{C}'$  correlation functions compared to the  $\mathbf{C}_E$  correlation functions is that the  $\mathbf{C}_E$  can be evaluated using every time step as a time origin, whereas a new time origin can only be selected once every  $\tau_s$  time units in the calculation of  $\mathbf{C}'$ .

The integrals of  $\mathbf{C}_E(t)$  and  $\mathbf{C}'(t)$  for  $\gamma=2.0$  are shown in Figs. 3 and 4. The integrals of all correlation functions

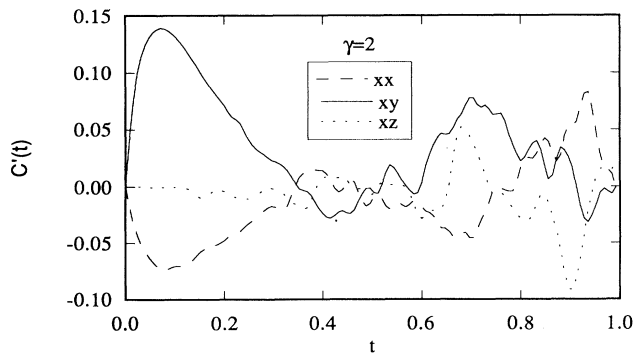


FIG. 2. Elements of the correlation function tensor  $\mathbf{C}'(t)$  at a strain rate of  $\gamma=2.0$ .

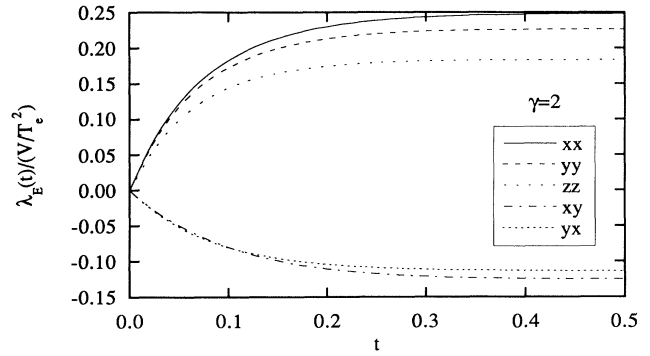


FIG. 3. Integrals of the nonzero diagonal and off-diagonal elements of the correlation function tensor  $\mathbf{C}_E(t)$  at a strain rate of  $\gamma=2.0$ . The values of the integrals were taken at a reduced time of 1.0, but they were well converged at  $t=0.5$ .

appear to have converged sufficiently by  $t=0.5$ . To remove the effect of the noisy tail on the  $\mathbf{C}'$  correlation functions, the value of  $\lambda'$  was taken from the integral at a time after the decay of the peak in the correlation function but before the increase in the noise (approximately  $t=0.4-0.5$ ).

The strain-rate dependences of the diagonal and off-diagonal elements of  $\lambda_E$  are shown in Figs. 5 and 6, respectively.  $\lambda_{xx}$ ,  $\lambda_{yy}$ , and  $\lambda_{zz}$  are independent of strain rate to within the errors up to  $\gamma=1.0$ . The average of the zero strain-rate values is  $7.33 \pm 0.05$ , in agreement with the results of the NEMD constant temperature simulations of Evans and the equilibrium Green-Kubo results mentioned previously. Note that long runs at zero shear and constant energy with the energy per particle set to  $-0.8979$  actually gave a kinetic temperature of 2.03, slightly higher than the target value of 2.00.

The only nonzero off-diagonal elements of  $\lambda_E$  are the  $xy$  and  $yx$  elements. The strain-rate dependences of  $\lambda_{xy}$  and  $\lambda_{yx}$  are clearly initially linear in  $\gamma$ .

The Lagrangian corrections to the thermal conductivity are shown in Fig. 7. Only the corrections to the  $xx$  and  $xy$  elements are shown, because all of the others are zero. The  $xx$  element is quadratic in  $\gamma$  and the  $xy$  element is linear in  $\gamma$ . Both corrections tend to reduce the magnitude of the corresponding elements of the thermal-

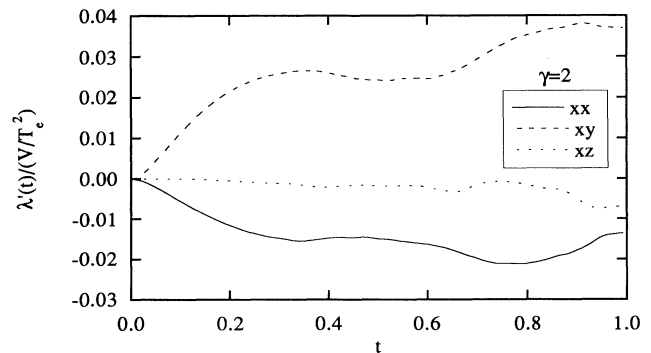


FIG. 4. Integrals of the diagonal and off-diagonal elements of the correlation function tensor  $\mathbf{C}'(t)$  at a strain rate of  $\gamma=2.0$ .

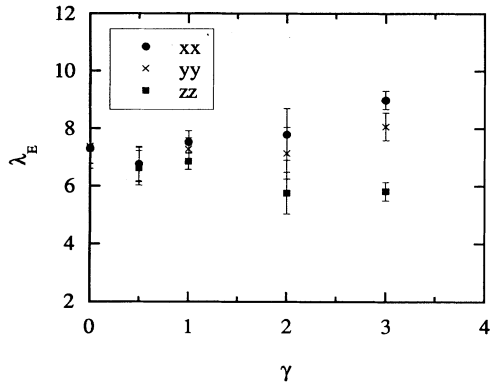


FIG. 5. Diagonal elements of the thermal-conductivity tensor  $\lambda_E$  as a function of strain rate  $\gamma$ .

conductivity tensor, with the result that the corrected value of  $\lambda_{xx}$  is closer to  $\lambda_{yy}$  and the corrected value of  $\lambda_{xy}$  is further from  $\lambda_{yx}$ , as shown in Figs. 8 and 9.

Symmetry arguments can provide some insight into the strain-rate dependence of the thermal-conductivity tensor. A fluid undergoing planar shear flow is symmetrical with respect to a rotation of  $\pi$  about the  $z$  axis. Application of this symmetry element to the general form of  $\lambda(\gamma)$  leads to  $\lambda_{xz} = \lambda_{yz} = \lambda_{zx} = \lambda_{zy} = 0$ , in agreement with our simulation results. The behavior of  $\lambda(\gamma)$  with respect to reversal of the shear can be found by the following method. The strain rate,  $\gamma = \partial u_x / \partial y$ , can be reversed by inverting either the  $x$  or the  $y$  axis. Considering inversion of the  $x$  axis first, we find that since  $J_x$  is inverted and  $\partial T / \partial y$  remains the same,  $\lambda_{xy}$  must be an odd function of  $\gamma$ . Likewise, we find that  $\lambda_{yx}$  is also odd in  $\gamma$ . Both  $J_x$  and  $\partial T / \partial x$  change sign on inversion of the  $x$  axis, so  $\lambda_{xx}$  must be even in  $\gamma$ . Inversion of the  $y$  axis leads to the conclusion that  $\lambda_{yy}$  is an even function of  $\gamma$ . Inversion of either the  $x$  or the  $y$  axis leaves the equation for  $J_z$  unchanged, so  $\lambda_{zz}$  must be an even function of  $\gamma$ . This analysis is valid for arbitrary values of  $\gamma$  and the conclusions are consistent with our simulation results. They should also hold for other vectorial processes such as

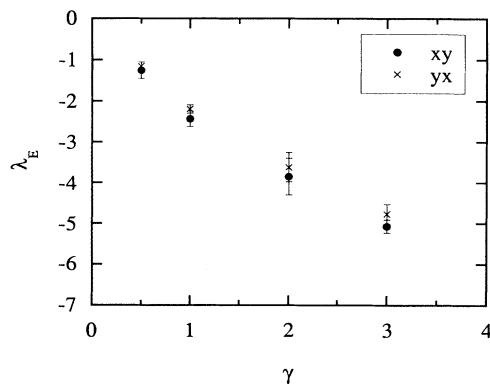


FIG. 6. Off-diagonal elements of the thermal-conductivity tensor  $\lambda_E$  as a function of strain rate  $\gamma$ .

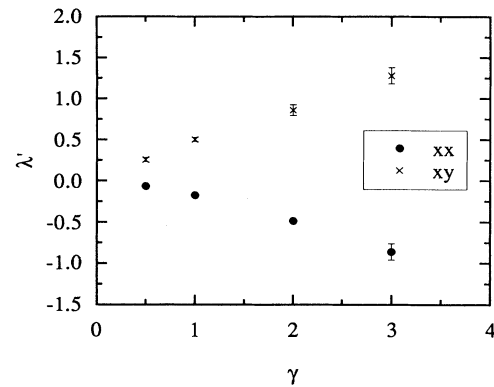


FIG. 7. Corrections to the  $xx$  and  $xy$  elements of the thermal-conductivity tensor as a function of strain rate  $\gamma$ .

diffusion in shear flow. This appears to be the case when previously obtained results for diffusion in shearing atomic fluids are examined [8].

The macroscopic constitutive equation [Eq. (10)] that we have used to define  $\lambda$  is a linear constitutive equation. The nonlinear dependence of the heat-flux vector on the strain rate has been absorbed into the strain-rate dependence of the thermal-conductivity tensor. One way of explicitly revealing the strain-rate dependence of the thermal-conductivity tensor is to expand the flux in terms of the strain rate and the temperature gradient about its value when the thermodynamic forces are zero. Of course this expansion is only valid if the flux is an analytic function of the forces and for small values of the forces. The question of analyticity is related to the existence of long-time tails in correlation functions. Near the critical point, the effects of long-time tails are pronounced. At low density, high-temperature state points, and for finite systems, the long-time tails may be sufficiently weak for analytic behavior to be observed. Furthermore, the long-time tail effect is much weaker for the heat-flux correlation function than it is for the velocity autocorrelation function or the stress autocorrelation function [7]. With these reservations in mind, we expand the heat flux as a truncated generalized Taylor series

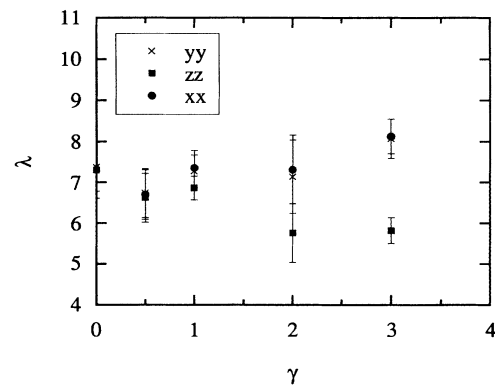


FIG. 8. Diagonal elements of the thermal-conductivity tensor  $\lambda$  as a function of strain rate  $\gamma$ , where the  $xx$  element has now been replaced by the corrected  $xx$  element.

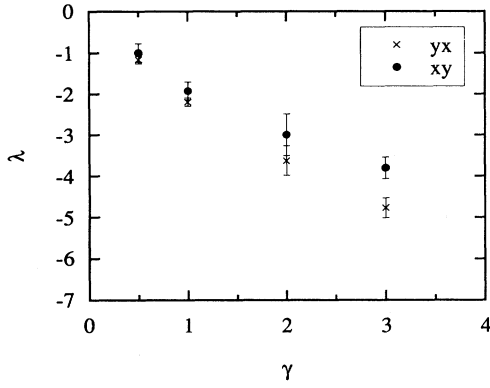


FIG. 9. Off-diagonal elements of the thermal-conductivity tensor  $\lambda$  as a function of strain rate  $\gamma$ , where the  $xy$  element has now been replaced by the corrected  $xy$  element.

$$\begin{aligned} \mathbf{J}(\mathbf{X}_1, \mathbf{X}_2) = & \mathbf{J}(0) + \sum_{i=1}^2 \frac{\partial \mathbf{J}}{\partial \mathbf{X}_i} \Big|_{x=0} \cdot \mathbf{X}_i \\ & + \frac{1}{2!} \sum_{i=1}^2 \sum_{j=1}^2 \frac{\partial^2 \mathbf{J}}{\partial \mathbf{X}_i \partial \mathbf{X}_j} \Big|_{x=0} : \mathbf{X}_i \mathbf{X}_j \\ & + \frac{1}{3!} \sum_{i=1}^2 \sum_{j=1}^2 \sum_{k=1}^2 \frac{\partial^3 \mathbf{J}}{\partial \mathbf{X}_i \partial \mathbf{X}_j \partial \mathbf{X}_k} \Big|_{x=0} \\ & (\cdot)^{[3]} \mathbf{X}_i \mathbf{X}_j \mathbf{X}_k . \end{aligned} \quad (18)$$

Note that the expansion is performed about the equilibrium state so we immediately see that  $\mathbf{J}(0)=0$ . As it is written, Eq. (18) involves only vector forces, but the generalization to arbitrary tensor forces is obvious. In the present case, the thermodynamic forces  $\mathbf{X}_1$  and  $\mathbf{X}_2$  represent the temperature gradient  $\nabla T$  and the strain-rate tensor  $\nabla \mathbf{u}$ . The standard linear constitutive relations of linear nonequilibrium thermodynamics are equivalent to Eq. (18) truncated at the linear term. However, it is instructive to look at the higher terms in order to determine the leading contributions due to the strain-rate tensor corresponding to planar Couette flow  $\nabla \mathbf{u} = \mathbf{j} \mathbf{j} \gamma$ . First, we consider the linear terms:

$$\sum_{i=1}^2 \frac{\partial \mathbf{J}}{\partial \mathbf{X}_i^{[n]}} \Big|_{x=0} (\cdot)^{[n]} \mathbf{X}_i^{[n]} = \mathbf{A}^{[2]} \cdot \nabla T + \mathbf{B}^{[3]} : \nabla \mathbf{u} . \quad (19)$$

The phenomenological coefficient tensors  $\mathbf{A}^{[2]}$  and  $\mathbf{B}^{[3]}$  are properties of the equilibrium fluid, and so must be isotropic tensors. The heat-flux vector and the temperature gradient are polar vectors, and the strain-rate tensor is also polar, so  $\mathbf{A}^{[2]}$  and  $\mathbf{B}^{[3]}$  must both be polar. The

only nontrivial isotropic second-rank tensor is the Kronecker or unit tensor so the first term on the right-hand side just reduces to the standard Fourier law for isotropic fluids. However, there are no nontrivial polar isotropic third-rank tensors, so the second term is zero (i.e., to linear order, a strain rate cannot generate a heat flow in an isotropic fluid). The symmetry considerations used so far are well known in linear nonequilibrium thermodynamics, and are collectively known as Curie's principle [1].

The terms resulting from the second-order partial derivatives can be written as

$$\begin{aligned} & \frac{1}{2!} \sum_{i=1}^2 \sum_{j=1}^2 \frac{\partial^2 \mathbf{J}}{\partial \mathbf{X}_i^{[n]} \partial \mathbf{X}_j^{[m]}} \Big|_{x=0} (\cdot)^{[n+m]} \mathbf{X}_i^{[n]} \mathbf{X}_j^{[m]} \\ & = \mathbf{C}^{[3]} : \nabla T \nabla T + \mathbf{D}^{[4]} (\cdot)^{[3]} \nabla T \nabla \mathbf{u} \\ & \quad + \mathbf{E}^{[4]} (\cdot)^{[3]} \nabla \mathbf{u} \nabla T + \mathbf{F}^{[5]} (\cdot)^{[4]} \nabla \mathbf{u} \nabla \mathbf{u} . \end{aligned} \quad (20)$$

The phenomenological coefficient tensors must be isotropic polar tensors, but all nontrivial isotropic tensors of odd rank are axial, which eliminates the third- and fifth-rank tensors  $\mathbf{C}$  and  $\mathbf{F}$ . A nonirreducible form of the general fourth-rank isotropic tensor can be formed from a linear combination of the three fourth-rank isotropic tensors giving

$$\mathbf{D}_{\alpha\beta\gamma\delta} = c_1 \delta_{\alpha\beta} \delta_{\gamma\delta} + c_2 \delta_{\alpha\gamma} \delta_{\beta\delta} + c_3 \delta_{\alpha\delta} \delta_{\beta\gamma} . \quad (21)$$

The tensor  $\mathbf{D}$  possesses intrinsic symmetry additional to the symmetry related to the isotropy of the material because of the equality of the partial derivatives

$$\frac{\partial^2 \mathbf{J}}{\partial \nabla T \partial \nabla \mathbf{u}} = \frac{\partial^2 \mathbf{J}}{\partial \nabla \mathbf{u} \partial \nabla T} . \quad (22)$$

This gives  $\mathbf{D} = \mathbf{E}$  and leads to the symmetry  $\mathbf{D}_{\alpha\beta\gamma\delta} = \mathbf{D}_{\beta\gamma\alpha\delta}$  which, when applied to Eq. (21), yields  $c_1 = c_2 = c_3$ . Now it is straightforward to show that

$$\mathbf{D} (\cdot)^{[3]} (\nabla T \nabla \mathbf{u} + \nabla \mathbf{u} \nabla T) = \mathbf{L}_1 \cdot \nabla T , \quad (23)$$

where  $\mathbf{L}_1$  is the second-rank tensor

$$\mathbf{L}_1 = \begin{bmatrix} 0 & 2c_1 \gamma & 0 \\ 2c_1 \gamma & 0 & 0 \\ 0 & 0 & 0 \end{bmatrix} . \quad (24)$$

The terms arising from the third-order derivatives can be treated in a similar way. Once again, we use the fact that the tensors of odd order are eliminated because there are no polar isotropic tensors of odd rank. Then we are left with

$$\begin{aligned} & \frac{1}{3!} \sum_{i=1}^2 \sum_{j=1}^2 \sum_{k=1}^2 \frac{\partial^3 \mathbf{J}}{\partial \mathbf{X}_i^{[n]} \partial \mathbf{X}_j^{[m]} \partial \mathbf{X}_k^{[l]}} \Big|_{x=0} (\cdot)^{[n+m+l]} \mathbf{X}_i^{[n]} \mathbf{X}_j^{[m]} \mathbf{X}_k^{[l]} = \mathbf{G}^{[4]} (\cdot)^{[3]} \nabla T \nabla T \nabla T + \mathbf{H}^{[6]} (\cdot)^{[5]} \nabla \mathbf{u} \nabla \mathbf{u} \nabla T \\ & \quad + \mathbf{J}^{[6]} (\cdot)^{[5]} \nabla \mathbf{u} \nabla T \nabla \mathbf{u} + \mathbf{K}^{[6]} (\cdot)^{[5]} \nabla T \nabla \mathbf{u} \nabla \mathbf{u} . \end{aligned} \quad (25)$$

We will only consider terms linear in the temperature gradient, so the term proportional to  $\nabla T \nabla T \nabla T$  will be ignored.

The general sixth-rank isotropic tensor is a linear combination of the 15 sixth-rank isotropic tensors and can be written as

$$\begin{aligned} H_{\alpha\beta\gamma\delta\epsilon\zeta} = & c_1 \delta_{\alpha\beta} \delta_{\gamma\delta} \delta_{\epsilon\zeta} + c_2 \delta_{\alpha\beta} \delta_{\gamma\epsilon} \delta_{\delta\zeta} + c_3 \delta_{\alpha\beta} \delta_{\gamma\zeta} \delta_{\delta\epsilon} + c_4 \delta_{\alpha\gamma} \delta_{\beta\delta} \delta_{\epsilon\zeta} + c_5 \delta_{\alpha\gamma} \delta_{\beta\epsilon} \delta_{\delta\zeta} + c_6 \delta_{\alpha\gamma} \delta_{\beta\zeta} \delta_{\delta\epsilon} \\ & + c_7 \delta_{\alpha\delta} \delta_{\beta\gamma} \delta_{\epsilon\zeta} + c_8 \delta_{\alpha\epsilon} \delta_{\beta\gamma} \delta_{\delta\zeta} + c_9 \delta_{\alpha\zeta} \delta_{\beta\gamma} \delta_{\delta\epsilon} + c_{10} \delta_{\alpha\delta} \delta_{\beta\epsilon} \delta_{\gamma\zeta} + c_{11} \delta_{\alpha\delta} \delta_{\beta\zeta} \delta_{\gamma\epsilon} \\ & + c_{12} \delta_{\alpha\epsilon} \delta_{\beta\delta} \delta_{\gamma\zeta} + c_{13} \delta_{\alpha\zeta} \delta_{\beta\delta} \delta_{\gamma\epsilon} + c_{14} \delta_{\alpha\epsilon} \delta_{\beta\zeta} \delta_{\gamma\delta} + c_{15} \delta_{\alpha\zeta} \delta_{\beta\epsilon} \delta_{\gamma\delta}. \end{aligned} \quad (26)$$

The partial derivatives defining the three sixth-rank tensors  $\mathbf{H}$ ,  $\mathbf{J}$ , and  $\mathbf{K}$  are equal, leading to the additional symmetry  $H_{\alpha\beta\gamma\delta\epsilon\zeta} = H_{\alpha\delta\epsilon\beta\gamma\zeta} = H_{\beta\gamma\alpha\delta\epsilon\zeta}$ . It is then straightforward to show that this implies that all constants  $c_1$  to  $c_{15}$  in Eq. (26) are equal. Then the third-order terms reduce to

$$\mathbf{H}(\cdot)^{[5]}(\nabla\mathbf{u}\nabla\mathbf{u}\nabla T + \nabla\mathbf{u}\nabla T\nabla\mathbf{u} + \nabla T\nabla\mathbf{u}\nabla\mathbf{u}) = \mathbf{L}_2 \cdot \nabla T, \quad (27)$$

where  $\mathbf{L}_2$  is a second-rank tensor given by

$$\mathbf{L}_2 = \begin{bmatrix} a\gamma^2 & 0 & 0 \\ 0 & a\gamma^2 & 0 \\ 0 & 0 & \frac{a}{3}\gamma^2 \end{bmatrix}. \quad (28)$$

Combining the above results, we see that the constitutive equation for heat flow in a shearing system with a linear velocity gradient can be written as

$$\mathbf{J} = -\lambda(\gamma) \cdot \nabla T, \quad (29)$$

with

$$\lim_{\gamma \rightarrow 0} \lambda(\gamma) = \begin{bmatrix} \lambda_0 + b\gamma^2 & a\gamma & 0 \\ a\gamma & \lambda_0 + b\gamma^2 & 0 \\ 0 & 0 & \lambda_0 + \frac{b}{3}\gamma^2 \end{bmatrix}, \quad (30)$$

where  $\lambda_0$  is the equilibrium thermal conductivity. This equation shows that the assumed Taylor series expansion combined with symmetry considerations will give strain-rate dependences of the type observed in these simulations. The initial strain-rate dependence of the thermal-conductivity tensor seen in Figs. 8 and 9 is consistent with Eq. (30) where  $b \approx 0$ , and  $a \approx -2.2$ . The form of the thermal-conductivity tensor given in Eq. (30) also shows that the principal axes of the thermal-conductivity tensor will be at  $45^\circ$  to the streamlines in the zero strain-rate limit.

Away from the zero strain-rate limit, the Taylor series expansion of the flux in terms of the forces is not expected to be valid and so there is no reason to expect Eq. (30) to hold.

## V. CONCLUSION

We have used the Green-Kubo relation for the thermal conductivity of a strongly shearing liquid with a weak temperature gradient recently derived by Evans [2] to

calculate the strain-rate-dependent thermal-conductivity tensor of a Lennard-Jones fluid. The nonequilibrium molecular-dynamics SIlod algorithm was used to simulate shearing steady states with fixed internal energy. We have found that the diagonal elements of the thermal-conductivity tensor were independent of the strain rate until  $\gamma = 1.0$ , after which the  $xx$  and  $yy$  elements increased weakly with  $\gamma$  and the  $zz$  element decreased weakly. Off-diagonal elements of the thermal-conductivity tensor were introduced because of the reduced isotropy of the sheared system compared to an equilibrium system. The  $xy$  and  $yx$  elements of the thermal-conductivity tensor were negative and decreased, initially linearly, with increasing strain rate. Symmetry arguments were used to show that the diagonal elements of the thermal-conductivity tensor must be even in the strain rate  $\gamma$ , while the off-diagonal elements must be odd in  $\gamma$ . Using a Taylor series expansion of the heat flux in terms of the temperature gradient and the strain rate, we found that the  $xy$  and  $yx$  elements of the thermal-conductivity tensor were linear in the strain rate and the  $xx$ ,  $yy$ , and  $zz$  elements of the thermal-conductivity tensor were quadratic in the strain rate in the zero strain-rate limit.

The anisotropy of the thermal-conductivity tensor for a shearing atomic fluid can be attributed to the anisotropy of the liquid structure induced by the shear. We found  $\lambda_{xy} / \frac{1}{3} \text{Tr}(\lambda) = -0.26\gamma$  below  $\gamma = 1.0$ , in reduced units. In real units, this becomes  $\lambda_{xy} / \frac{1}{3} \text{Tr}(\lambda) = -5.6 \times 10^{-13} \gamma$  for argon, with  $\gamma$  expressed in Hz. The largest strain rates that are easily attainable experimentally are of the order of  $10^4$  Hz, making the anisotropy unmeasurably small for argon at the state point we have considered. In more complex molecular fluids, an additional mechanism for anisotropy of the thermal-conductivity tensor exists—shear-induced orientation. Experimental studies of the thermal conductivity of complex fluids such as polymer melts have shown that the strain-rate dependence of the thermal conductivity is measurable [10,11]. The anisotropy of the thermal-conductivity tensor is expected to be similar to that of the order tensor [10]. In future work, we intend to calculate the thermal-conductivity tensor for shearing molecular fluids.

## ACKNOWLEDGMENT

We wish to thank the Australian National University Supercomputer Facility for a generous grant of computer time on the University's Fujitsu supercomputers.

- [1] S. R. de Groot and P. Mazur, *Nonequilibrium Thermodynamics* (North-Holland, Amsterdam, 1962).
- [2] D. J. Evans, *Phys. Rev. A* **44**, 3630 (1991).
- [3] D. J. Evans, A. Baranyai, and S. Sarman, *Mol. Phys.* **76**, 661 (1992).
- [4] J. P. Hansen and I. R. McDonald, *Theory of Simple Liquids* (Academic, London, 1986).
- [5] D. J. Evans and G. P. Morris, *Statistical Mechanics of Nonequilibrium Liquids* (Academic, London, 1990).
- [6] A. Baranyai and D. J. Evans, *Mol. Phys.* **70**, 53 (1990).
- [7] D. J. Evans, *Phys. Rev. A* **34**, 1449 (1986).
- [8] S. Sarman, D. J. Evans, and A. Baranyai, *Phys. Rev. A* **46**, 893 (1992).
- [9] D. J. Evans and S. Sarman, *Phys. Rev. E* **48**, 65 (1993).
- [10] B. Chitragad and J. J. C. Picot, *Polym. Eng. Sci.* **21**, 782 (1981).
- [11] A. Dutta and R. A. Mashelkar, *Adv. Heat Transfer* **18**, 161 (1987).